

Alternative way to locate the transition temperatures of polymeric models with loops

H. A. Lim and D. E. Burnette

Supercomputer Computations Research Institute, Florida State University, Tallahassee, Florida 32306-4052

(Received 5 July 1989)

We investigate a new criterion that can be used to locate the transition temperatures of walk models and apply the criterion to locate the transition temperatures of trails and silhouettes on a square, a triangular, a simple cubic, and a face-centered-cubic lattice. As the temperature is varied, it is observed that the odd moments or the reduced moments of the persistence lengths undergo a drastic change in a narrow temperature range. The criterion exploits this interesting observation and identifies the drastic change with a collapse of the walk configurations from the swollen phase to the compact phase. The transition temperatures obtained from this criterion for trails on the square, triangular, simple cubic, and face-centered-cubic lattice are, respectively, 1.1, 0.4, 0.6, and 0.3; and for the silhouettes they are, respectively, 1.9, 1.2, 1.4, and 0.9. The results for trails on the square and simple cubic lattices are very close to those of existing computer-simulation results of much longer chains (~250).

I. INTRODUCTION

In two previous papers^{1,2} (henceforth referred to as papers I and II), we study the persistency properties of two polymeric models with loops—trails³⁻¹⁶ and silhouettes^{1,2,9,10}—on two-dimensional (2D) and three-dimensional (3D) lattices. Trails are walks which are allowed to intersect, but are not allowed to overlap their own path; silhouettes, on the other hand, are just the shadows of trails. By introducing a tunable fugacity factor $f = e^{\Theta} = e^{-|\epsilon|/k_B T}$, where ϵ is the energy associated with an intersection, the number of intersections can be controlled and the behavior of the averaged persistence lengths as a function of the temperature can be studied. Interpreting in terms of the fugacity factor, the usual self-avoiding walks¹⁷ (SAW's) correspond to the class of trails at $\Theta = -\infty$, and the usual Malakis trails is the class of trails at $\Theta = 0$.^{3,4,12} In the extreme case of $\Theta = +\infty$, there is a preponderance for walk configurations with the maximal number of intersections, so that the usual random walks¹⁸ (RW's), in which overlaps are allowed, are closely mimicked but are never fully modeled. These four walk models and their respective constraints are illustrated in Fig. 1.

To date, the only rigorous analysis of trails deals with trails on hexagonal lattice (coordination number $q=3$).¹⁵ But on a hexagonal lattice, trails and SAW's are almost equivalent.¹¹⁻¹³ In the former, self-intersections are not possible except at the origin, or the configuration must terminate at an already visited site. Figure 1 illustrates such an example: bond 6 self-intersects at the origin O ; if bond 11 has ended at site a , the trail configuration must terminate for bond overlaps are forbidden. On lattices with higher coordination numbers, trails can also self-intersect at an already visited site. This introduces richer features into the model, and can lead to quite different thermodynamical behaviors. It is thus seen that numerical studies of the trail model on lattices with $q > 3$ are still desirable.

We shall also study silhouettes. Silhouettes, as first introduced by one of the authors, have been shown to be in a distinct universality class from that of trails.^{9,10} This itself furnishes a motivation for studying the silhouette model. It should be recalled that on a hexagonal lattice, the self-interactions are only of two types: a self-interaction at the origin or a terminating self-

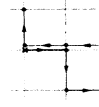
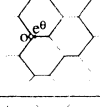
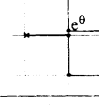
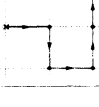
WALKS	SITE INTERSECTION	BOND OVERLAP	POSSIBLE CONFIGURATIONS	
RW	✓	✓		
TRAIL	✓	X		
SILH-OUETTE	✓	X		
SAW	X	X		

FIG. 1. The four types of walks on regular lattices: random walks (RW), trails, silhouettes, and self-avoiding walks (SAW), and their respective constraints. In each walk, a possible configuration is given on each of the two lattices: hexagonal and square. By comparing the configurations, it is easy to see that on the hexagonal lattice, trails and silhouettes are identical, and are equivalent to SAW, except that trails and silhouettes can self-intersect at the origin or terminate at an already visited site.

intersection. Because of this restriction, trails and silhouettes are identical on this lattice. On lattices with $q > 3$, the self-intersections can be of a crossing type or of an osculating type; an example of each is given in Fig. 2. This leads to a multiplicity of trails for each silhouette in lattices with $q > 3$. This also introduces more features and differentiates the trail model from the silhouette model.

By the very definition, trails (which are directional) may describe polymers in which the order of the building bonds are important, e.g., copolymers. On the other hand, silhouettes, (which are nondirectional) may describe polymers in which the order of the building bonds are unimportant, e.g., homopolymers.^{19–22} As the temperature is increased via the tunable fugacity factor ($f = e^{-|e|/k_B T}$), the trail and silhouette walk configurations undergo a transition from a swollen phase to a collapsed phase (at their respective transition temperatures). In the terminology of a polymer in a solvent, this transition corresponds to the fact that as the solvent worsens, the monomer-monomer attractions become more effective and at the transition temperature, the attractions cancel the excluded volume repulsions so that the polymer as a whole collapses.

Papers I and II provide extensive systematic studies of the important concept of persistence lengths on square ($q=4$), triangular ($q=6$), simple cubic ($q=6$), and face-centered-cubic ($q=12$) lattices. The papers also present for the first time persistence lengths organized according to the number of intersections and the path lengths of the configurations. The observation of a sudden collapse in the averaged odd moments of the persistence lengths, as the temperature is varied, is further reported in these papers. The current paper is prompted by this interesting observation.

In this paper we intend to explore this sudden collapse and, in particular, we shall investigate the possibility of a new criterion to locate the transition temperatures of the

trail model and the silhouette model. This temperature may be identified with or viewed as the temperature at which a polymeric chain undergoes a dramatic phase transition to the collapsed phase. Many biological, chemical, and physical systems capitalize on this sudden change in volume,^{20,23} for example, the collapse transition of DNA. Hence an accurate determination of this temperature is of practical importance. The usual approaches to locate the transition temperature make use of the concepts of the radii of gyration, the end-to-end distances, and the specific heats of the system in question.^{7–13} In this paper we intend to show how this important temperature can also be located using the averaged odd moments of the persistence lengths or the averaged odd reduced moments of the persistence lengths, which was first introduced in Refs. 20, 24, and 25 and was extended by Redner, Privman, and Considine.^{26,27}

A particularly interesting conclusion to emerge from studying walks on lattices is the concept of *universality* and *convergence*. Certain physical properties of walks depend only on the dimensionality of the space in which the lattice is embedded, and not on the lattice structure. Such properties are termed universal properties. Otherwise, the properties are nonuniversal. If in a given dimensionality, two walks have the same universal properties, they are said to belong to the same universality class. Otherwise, they are in distinct universality classes. In view of the fact that computer enumerations are just techniques used to study properties of polymers in solvents, it is thus also legitimate to ask the question that in a given dimensionality, which lattice (e.g., loose-packed versus close-packed) will converge faster to give reliable results. We thus investigate the criterion to locate the transition temperatures on square ($D=2$ and loose-packed), triangular ($D=2$ and close-packed), simple cubic ($D=3$ and loose-packed), and face-centered-cubic lattice ($D=3$ and close-packed). This will serve to test the *universality* and *convergence* properties on these lattices.

In Sec. II we shall recall some of the definitions of the thermodynamical functions, paving the way for Sec. III, in which it is shown, both analytically and numerically, how the transition temperature can be located via the averaged persistence lengths. Section IV gives the analysis of the 2D data and the corresponding analysis of the 3D data is given in Sec. V. Section VI contains the conclusion and discussion of the present findings.

II. THERMODYNAMIC FUNCTIONS

If $C(l, I, r)$ is the total number of trails (silhouettes) of chain length l with I intersections and end-to-end distance r , the partition function $Z_l(\Theta)$ on the lattice is then defined as^{1,2,7–10}

$$Z_l(\Theta) = \sum_{I \geq 0, r} C(l, I, r) e^{I\Theta}. \quad (1)$$

If the persistence length is induced by fixing the first step along a fixed direction,^{1,2,9,24–27} which we shall denote generically by \hat{x} , the averaged odd moments of the persistence lengths are then, by definition,^{1,2,9}

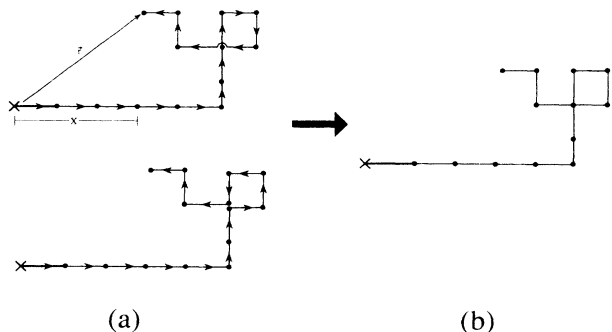


FIG. 2. (a) The two types of self-intersections in trails: a crossing self-intersection (top) and an osculating self-intersections (bottom); (b) the silhouette of the two trails in (a). As a consequence of the difference in the types of self-intersection, a silhouette can have a multiplicity of topologically nontrivial trails.

$$\langle X_l^{2k+1}(\Theta) \rangle \equiv \frac{\sum_{l,r} x^{2k+1}(l,I,r)C(l,I,r)e^{l\Theta}}{Z_l(\Theta)}$$

$$= \frac{\sum_l X^{2k+1}(l,I)e^{l\Theta}}{Z_l(\Theta)}, \quad k=0,1,\dots \quad (2)$$

We shall concentrate only on the averaged odd moments because they provide a natural way to quantify any asymmetry in the displacement distribution induced by the initial perturbation.²⁶ It has been shown, both numerically and heuristically, that^{1,2,9,26,27}

$$\langle X_l^{2k+1}(\Theta) \rangle = \begin{cases} A_0(\Theta)f(l) & \text{if } k=0 \\ A_k(\Theta)l^{pk\nu(\Theta)}f(l) & \text{if } k=1,2,\dots, \end{cases} \quad (3)$$

$$f(l) = \begin{cases} \ln(l) & \text{if } D=2 \\ \text{const} & \text{if } D=3, \end{cases}$$

where $\ln(\cdot) \equiv \log_e(\cdot)$ is the natural logarithm of the argument, p ($=2.0$) is a parameter, $\nu(\Theta)$ is the correlation exponent, and $A_k(\Theta)$ are the amplitudes. Any possible temperature dependence has been explicitly written out.

From the functional form of $\langle X_l^{2k+1}(\Theta) \rangle$, it is useful to introduce the averaged odd reduced moments of the persistence lengths. These are defined as^{1,2,9,27,28}

$$\langle M_l^{2k+1}(\Theta) \rangle = \frac{\langle X_l^{2k+1}(\Theta) \rangle}{\langle X_l(\Theta) \rangle}$$

$$= \frac{A_k(\Theta)}{A_0(\Theta)} l^{pk\nu(\Theta)}. \quad (4)$$

The latter expression has the advantage that it is $f(l)$ independent. This is especially important in cases where the chain lengths studied are relatively short, and the function $f(l)$ is a weak function of l , e.g., $f(l) \sim \ln l$ or l^w , $0 < w \ll 1$, the presence of which is very difficult to detect.

III. LOCATION OF TRANSITION TEMPERATURE

In this section we shall show how the transition temperature can be located from the averaged odd moments of the persistence lengths or the averaged odd reduced moments. Figure 3 illustrates some representative plots of $\langle X_l^{11}(\Theta) \rangle$ versus Θ from trails and silhouettes on a triangular lattice. Similar behaviors are also observed on the other three lattices. The sudden collapse of the averaged moments of the persistence lengths is very indicative of the possible existence of points of inflection. This suggests a derivation of Eq. (3) with respect to the inverse temperature Θ to locate these points of inflection.

A. Analytical treatment

We shall first show how to obtain these points of inflection from the rigorous expressions for $\langle X_l^{2k+1}(\Theta) \rangle$ or $\langle M_l^{2k+1}(\Theta) \rangle$. A derivation with respect to Θ yields

$$\frac{1}{\langle X_l^{2k+1}(\Theta) \rangle} \frac{\partial}{\partial \Theta} \langle X_l^{2k+1}(\Theta) \rangle = \frac{\partial}{\partial \Theta} \ln A_k(\Theta) + pk \frac{\partial}{\partial \Theta} \nu(\Theta) \ln l, \quad (5a)$$

$$\frac{1}{\langle M_l^{2k+1}(\Theta) \rangle} \frac{\partial}{\partial \Theta} \langle M_l^{2k+1}(\Theta) \rangle = \frac{\partial}{\partial \Theta} \ln \frac{A_k}{A_0}(\Theta) + pk \frac{\partial}{\partial \Theta} \nu(\Theta) \ln l. \quad (5b)$$

Equation (5) is easily simplified if we recall that in the infinite l limit, $\nu(\Theta)$ varies with the Θ like^{7-10,23}

$$\nu(\Theta) = \begin{cases} \nu_{\text{SAW}} & \text{if } \Theta < \Theta_t \\ \nu_t & \text{if } \Theta = \Theta_t \\ \nu_c & \text{if } \Theta > \Theta_t. \end{cases} \quad (6)$$

This is shown pictorially in Fig. 4. ν_{SAW} is the self-avoiding walk correlation exponent, ν_t is the correlation

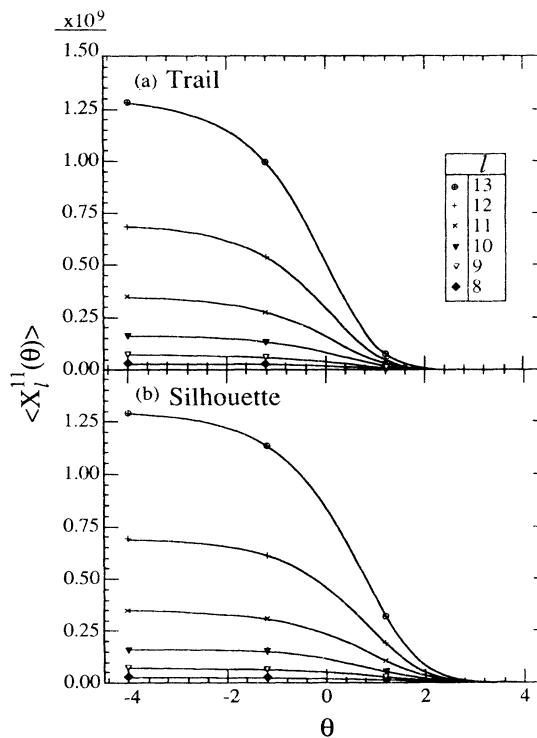


FIG. 3. (a) The averaged 11th moment of the persistence length of trails on a triangular lattice $\langle X_l^{11}(\Theta) \rangle$, plotted against the inverse temperature Θ ; and (b) the corresponding plot for silhouettes on a triangular lattice. There is a drastic change in the value of $\langle X_l^{11}(\Theta) \rangle$ within a narrow range of Θ . The units of lengths are in units of the lattice spacings, i.e., the ordinates are scaled dimensionless quantities (since the lattice spacing is set to unity). The units of the abscissas are in units of the intersection energy, i.e., the abscissas are scaled dimensionless temperatures (since the intersection energy is also set to unity).

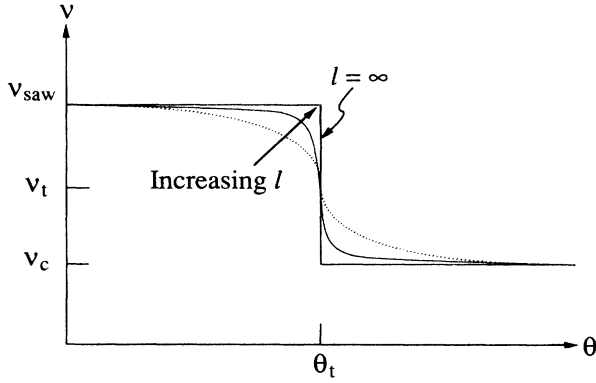


FIG. 4. Schematic plot to show how the correlation exponent $\nu(\Theta)$ varies with Θ . For finite chain length l , the transition at Θ_t is quite smooth. As l increases, the transition at Θ_t becomes steeper until in the $l = \infty$ limit, it becomes a step function. ν is a dimensionless parameter and Θ is the scaled dimensionless temperature.

exponent at the transition point, and ν_c is the correlation exponent in the collapse region. Thus, mathematically, $\nu(\Theta)$ can be expressed in terms of the Heaviside step function $H(\Theta - \Theta_t)$ as²⁹

$$\nu(\Theta) = \nu_{\text{SAW}} - (\nu_{\text{SAW}} - \nu_c)H(\Theta - \Theta_t), \quad (7)$$

$$H(\Theta - \Theta_t) = \begin{cases} 1 & \text{if } \Theta \geq \Theta_t \\ 0 & \text{if } \Theta < \Theta_t \end{cases}.$$

Thus

$$\frac{1}{\langle X_l^{2k+1}(\Theta) \rangle} \frac{\partial}{\partial \Theta} \langle X_l^{2k+1}(\Theta) \rangle \sim pk[-(\nu_{\text{SAW}} - \nu_c)\delta(\Theta - \Theta_t)] \ln l, \quad (8)$$

and a similar expression for the derivation of $\langle M_l^{2k+1}(\Theta) \rangle$. $\delta(\Theta - \Theta_t)$ is the usual Dirac δ function. Consequently, the derivatives vanish except at the transition temperature Θ_t .

B. Treatment of numerical data

To see how the analogs of Eq. (8) can be obtained for the numerical data, we have to go back to the defining equation, Eq. (2). A derivation with respect to Θ leads to

$$\frac{\partial}{\partial \Theta} \langle X_l^{2k+1}(\Theta) \rangle = \langle X_l^{2k+1}(\Theta)I(\Theta) \rangle - \langle X_l^{2k+1}(\Theta) \rangle \langle I(\Theta) \rangle. \quad (9)$$

Similarly, the averaged reduced moment and its derivative are, respectively,

$$\langle M_l^{2k+1}(\Theta) \rangle = \frac{\sum_{l,r} x^{2k+1}(l,I,r)C(l,I,r)e^{I\Theta}}{\sum_{l,r} x(l,I,r)C(l,I,r)e^{I\Theta}}, \quad (10a)$$

and

$$\frac{\partial}{\partial \Theta} \langle M_l^{2k+1}(\Theta) \rangle = \frac{\langle X_l^{2k+1}(\Theta)I(\Theta) \rangle}{\langle X_l(\Theta) \rangle} - \frac{\langle X_l^{2k+1}(\Theta) \rangle \langle X_l(\Theta)I(\Theta) \rangle}{\langle X_l(\Theta) \rangle \langle X_l(\Theta) \rangle}. \quad (10b)$$

Equations (9) and (10) can be equated to their respective analytical analogs of Eq. (8).

IV. ANALYSIS OF 2D NUMERICAL DATA

The total number of trails (silhouettes), and their persistence lengths on the 2D square and triangular lattices have been given elsewhere,^{1,2,7,8,10} we shall not reproduce them here. Since our numerical data are obtained from exact enumerations and the chain lengths are relatively short, the data will not be sufficiently accurate to detect the presence of the $\ln l$ dependence of $\langle X_l^{2k+1}(\Theta) \rangle$. We will thus analyze the 2D data using both the moments $\langle X_l^{2k+1}(\Theta) \rangle$ and the reduced moments $\langle M_l^{2k+1}(\Theta) \rangle$, but with emphasis on the reduced moments.

A. Square lattice

Figure 5 depicts plots of $-(\partial/\partial\Theta)\langle M_l^5(\Theta) \rangle$ and $-(\partial/\partial\Theta)\langle M_l^9(\Theta) \rangle$ against Θ from trails and silhouettes on a square lattice for $13 \leq l \leq 20$. The figures clearly bear out the fact that there is a sharp maximum for each l , and that as l increases, the peaks sharpen, showing that as $l \rightarrow \infty$, the peaks will tend to a δ function, as predicted in Eq. (8). Two interesting features are quite apparent: (a) the value of Θ at which the maximum occurs, Θ_{max} , tends toward a lower value as l increases; (b) as k increases, Θ_{max} also tends to a lower value. In Fig. 6a, Θ_{max} are plotted as a function of $1/l$ for trails and silhouettes. For a fixed k , it is seen that as l increases, Θ_{max} tends to a lower value in a regular trend and tends to an asymptotic limit. Figures 7(a) and 7(b) are similar plots using $k=2$ including the data from all four lattices. For the square lattice trails, Θ_{max} tends to the value ~ 1.1 in the $l \rightarrow \infty$ limit. The corresponding value for silhouettes is $\Theta_{\text{max}} \sim 1.9$. In Figs. 8(a) and 8(b), Θ_{max} are plotted against k . The shift toward a lower value in Θ_{max} as k increases is very apparent, and for a constant k , the rate of shift diminishes as l increases. This rate is expected to vanish in the $l = \infty$ limit.

Even though the square lattice is loosely packed, odd-even oscillations are not observed in Figs. 6 and 7, unlike the determination of the transition temperature from the specific heats.^{8,10} The transition temperature obtained from the reduced moments of the persistence lengths is ~ 1.0 for trails, ~ 1.8 for silhouettes. These values are lower than those obtained from the specific heats in exact enumeration ($\Theta \sim 1.5$ and ~ 2.5 , respectively).^{8,10} In fact, the transition temperature for trails determined from the reduced moments comes very close to that obtained by the scanning method,¹¹⁻¹³ where walks of $l \leq 220$ are used. This provides support for our current results.

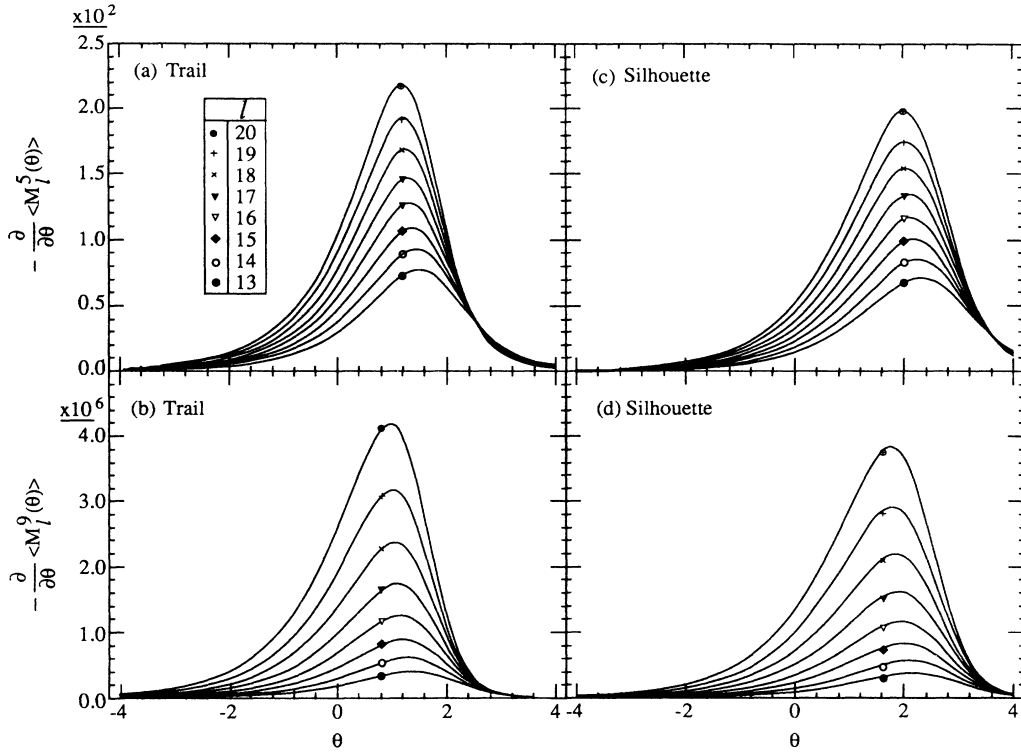


FIG. 5. (a) A representative plot of $-\frac{\partial}{\partial\Theta}\langle M_l^{2k+1}(\Theta)\rangle$ with $k=2$ and $l=13-20$ for trails on a square lattice; (b) the corresponding plot, but for $k=4$; (c) the corresponding plot of (a) for silhouettes; and (d) the corresponding plot of (b) for silhouettes. In each case, the plots show sharp maxima. As k increases for a fixed l , the values of Θ at the maxima Θ_{\max} , tend toward lower Θ . As l increases for a constant k , Θ_{\max} also show a regular shifting trend to lower values. The ordinates are scaled dimensionless quantities and the abscissas are the scaled temperatures.

B. Triangular lattice

Similar behaviors in $-\frac{\partial}{\partial\Theta}\langle M_l^{2k+1}(\Theta)\rangle$ as those observed in the square lattice (Fig. 5) are also observed in the triangular lattice. The Θ_{\max} are plotted versus $1/l$ in Fig. 6(b). From Figs. 7(a) and 7(b), the transition temperatures for trails and silhouettes are, respectively, $\Theta \sim 0.4$ and ~ 1.2 . Again these values are respectively lower than ~ 1.2 and ~ 1.67 , the transition temperatures for trails and silhouettes obtained via the specific heats.^{7,10}

Figures 8(c) and 8(d) present the plots of Θ_{\max} versus k for trails and silhouettes. Along the trajectory of constant k , the rate of shift of Θ_{\max} decreases and is expected to go to zero in the large- l limit also.

It is also seen that though the triangular lattice is closely packed, the Θ_{\max} in specific heats show a slight odd-even oscillation (though less severe than in a square lattice).^{7,10} In the case of the Θ_{\max} obtained from the reduced moments of persistence lengths, these oscillations are clearly absent.

C. Analysis using moments

The 2D data from the square lattice and the triangular lattice are also analyzed using the moments (rather than

the reduced moments). The Θ_{\max} are found to be on the average 0.3 ($\delta\Theta \sim 0.3$) lower than those obtained from the reduced moments. This is not surprising. As has been noted in paper I, when the moments are used, a slightly higher $\nu(\Theta)$ is obtained. From Fig. 4, we see that as $\nu(\Theta)$ is increased, Θ decreases, and this may explain the observed lower Θ values. Furthermore, as l increases, the slope in Fig. 4 becomes steeper, accounting for the diminishing rate of shift in Fig. 8.

The observation of the regular decreasing trend in Θ_{\max} and the clustering of Θ_{\max} as k increases may also be similarly explained. Our chain lengths are relatively short ($l \leq 20$ on the square lattice and $l \leq 13$ on the triangular lattice), so chain stiffness may tend to increase the persistence lengths [Eqs. (3) and (4)], which in turn show up as an increased $\nu(\Theta)$, and consequently lowering Θ_{\max} . As k increases, this effect is amplified. Since Θ_i is approached from $\Theta > \Theta_i$, we see that the clustering effect is a direct consequence of the “uphill climb” as Θ approaches Θ_i .

V. ANALYSIS OF 3D NUMERICAL DATA

The total number of trails (silhouettes), and their persistence lengths on the 3D simple cubic lattice and the

3D face-centered-cubic lattice have also been given elsewhere.^{1,2,8-10} We shall not reproduce them again.

Since in 3D $\langle X_l^{2k+1}(\Theta) \rangle$ scale with $f(l)=\text{const}$ [Eq. (3)], we shall analyze the moments of persistence lengths $\langle X_l^{2k+1}(\Theta) \rangle$, with less emphasis on the reduced moments $\langle M_l^{2k+1}(\Theta) \rangle$.

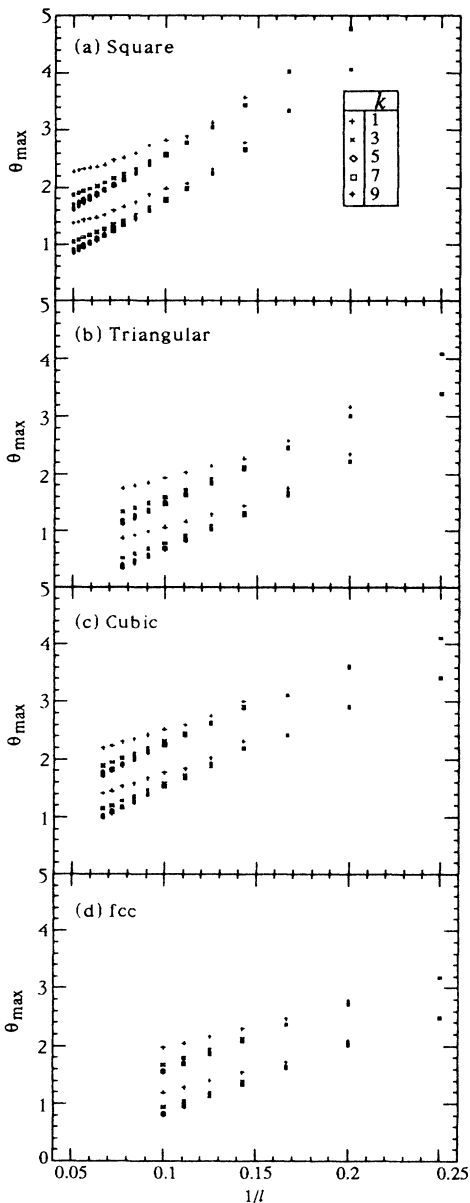


FIG. 6. (a) Plots of Θ_{\max} vs $1/l$ at various k values for trails and silhouettes on a square lattice; (b) the corresponding plots for trails and silhouettes on a triangular lattice; (c) the corresponding plots for trails and silhouettes on a simple cubic lattice; and (d) the corresponding plots for trails and silhouettes on a face-centered-cubic lattice. In each case, the upper set is for silhouettes and the lower set is for trails. Θ is the scaled dimensionless temperature and the abscissas are in units of inverse lattice spacings, which is set to unity.

A. Simple cubic lattice

Plots of $-(\partial/\partial\Theta)\langle X_l^{2k+1}(\Theta) \rangle$ versus Θ show similar behaviors as those observed in Fig. 5: flat tails and sharp maxima, with a regular shift toward lower Θ as l increases. Θ_{\max} are extracted from these plots and are plotted in Figs. 6(c) and 7. The transition temperature (Θ_{\max} extrapolated to $1/l=0$ in Fig. 6) is ~ 0.6 for trails and ~ 1.4 for silhouettes. These values should be contrasted with those obtained from the specific heats (~ 1.6 and ~ 2.6 , respectively).^{8,10} Preliminary results obtained from the scanning method for trails of chain length $l \leq 250$ show that $0.5 \leq \Theta_l \leq 0.6$.³⁰ This preliminary result is very close to what we obtained using the new approach.

Figures 9(a) and 9(b) are plots of Θ_{\max} as a function of k . Trends like those observed in 2D are also seen here and we shall not elaborate further. As in 2D, odd-even oscillations are not seen in the moments of persistence lengths analysis, even though the simple cubic lattice is loosely packed.

B. Face-centered-cubic lattice

In this lattice the derivative of the moments of the persistence lengths $-(\partial/\partial\Theta)\langle X_l^{2k+1}(\Theta) \rangle$ also show maxi-

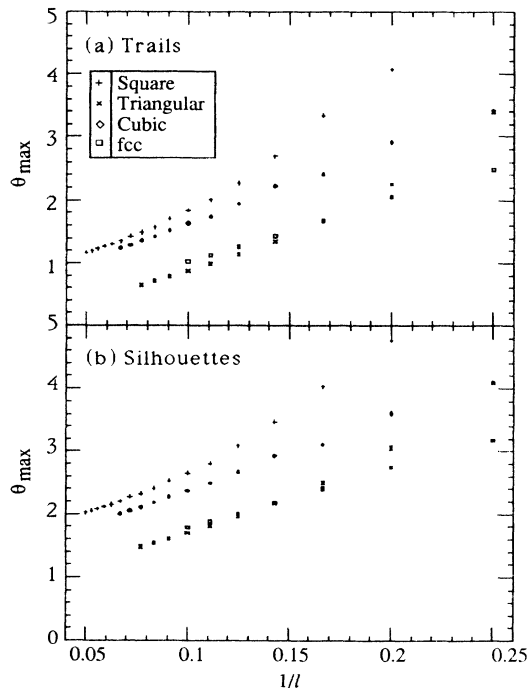


FIG. 7. (a) Plots similar to that in Fig. 6, but for a particular value of $k=2$, and for trails on all the four lattices for easy comparison; and (b) the corresponding plots, but for silhouettes on all four lattices. It is interesting to note that the transition temperatures (Θ_{\max} at $1/l=0$) in descending order are square, simple cubic, face-centered-cubic, and triangular. See text for a plausible explanation. The units on either axes are the same as those in Fig. 6.

ma as predicted in Eq. (8), and similar to those in Fig. 5. Plots of Θ_{\max} against $1/l$ are given in Figs. 6(d) and 7. The transition temperatures, as extrapolated from these plots (Fig. 6), are ~ 0.3 and ~ 0.9 for trails and silhouettes, respectively. These are lower than those predicted from the specific heats in exact enumerations (~ 1.2 and ~ 2.3 for trails and silhouettes, respectively).⁹

Other plots [Figs. 9(c) and 9(d)] show behaviors very similar to those observed on other lattices.

Though our chains are relatively short ($l \leq 10$), the results are quite stable and the plots are quite smooth. This is expected of most close-packed lattices, of which a face-centered-cubic lattice is one.

C. Analysis using reduced moments

The 3D data are also analyzed using the reduced moments. The corresponding Θ_{\max} are found to be only

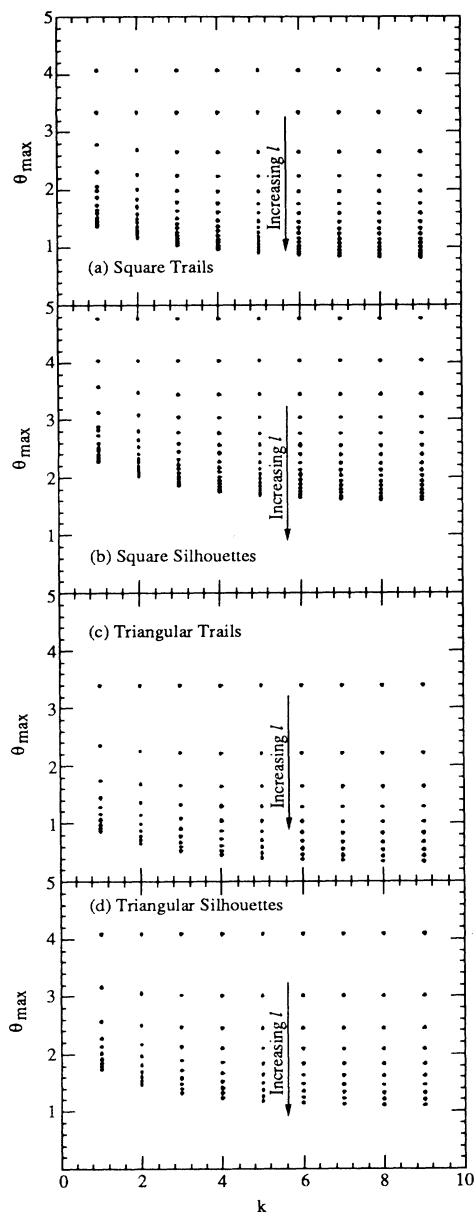


FIG. 8. (a) Plots of Θ_{\max} vs k for trails on a square lattice; (b) similar plot for silhouettes on a square lattice; (c) similar plots for trails on a triangular lattice; and (d) similar plots for silhouettes on a triangular lattice. The ordinates are the scaled dimensionless temperatures and the abscissas are dimensionless parameters.

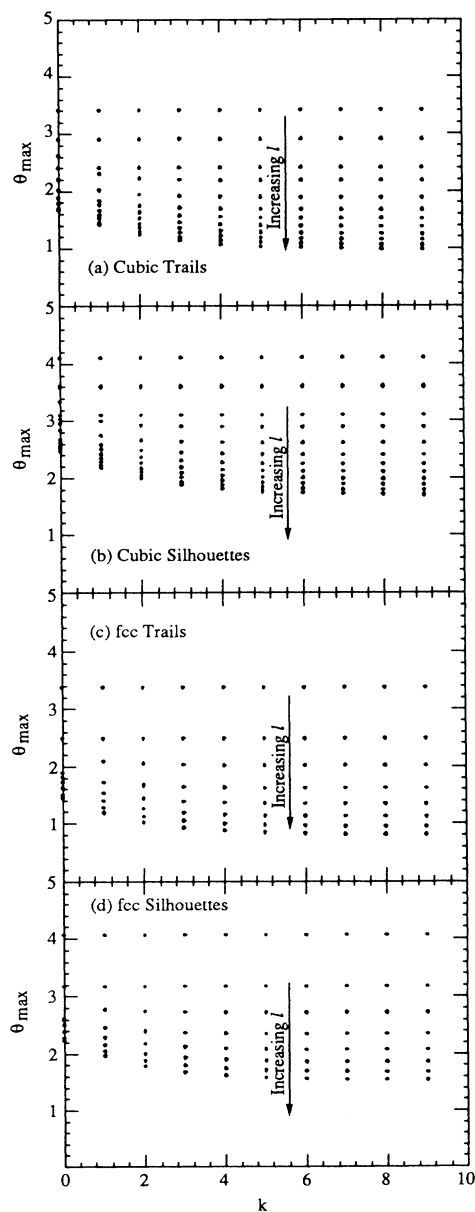


FIG. 9. Plot similar to those in Fig. 8, but for (a) trails and (b) silhouettes on a simple cubic lattice; and for (c) trails and (d) silhouettes on a face-centered-cubic lattice. The units on either axes are the same as those in Fig. 8.

slightly higher ($\delta\Theta \sim 0.1$) than those extracted from the moments. This may be taken as an evidence for the fact that $f(l) = \text{const}$, in agreement with the prediction of Eq. (3).^{26,27}

Though the $\delta\Theta$ in 3D is much smaller than the $\delta\Theta$ in 2D, the observed shifting trends in Θ_{max} as a function of l or k are equally prominent in 3D. A plausible explanation is the stiffness effects, as explained in 2D. But one thing is apparent in Figs. 7(a) and 7(b). In both 2D and 3D, the trails and the silhouettes on the more closely packed lattices (triangular lattice and face-centered-cubic lattice) always have a lower transition point. This is intuitively correct, for on these more closely packed lattices, the configurations have more flexibility and they can collapse at a higher temperature (or lower Θ). This fact is further substantiated by the fact that lattices with smaller included angles³¹ between adjacent bonds have lower transition temperatures. On closer scrutiny of Figs. 7(a) and 7(b), it is revealed that the transition temperatures, in descending order, are square, simple cubic, face-centered-cubic, and triangular. On a square lattice, the included angle is 90° ; on a simple cubic lattice, the included angle is also 90° ; on a face-centered-cubic lattice, the included angles are 60° and 90° , whereas on a triangular lattice, the included angle is 60° . The observed order is thus explained. Higher dimensionality will also allow for more flexibility. This is reflected in the square-lattice and the cubic-lattice case (same included angles); but in the case of the triangular lattice and the face-centered-cubic lattice, the higher dimensionality effect in the face-centered-cubic lattice compensates for the smaller included angle effect in the triangular lattice. Thus trails and silhouettes on these lattices have transition temperatures close to each other.

VI. CONCLUSION AND DISCUSSIONS

In the present paper we study the behavior of $\langle X_l^{2k+1}(\Theta) \rangle$ or $\langle M_l^{2k+1}(\Theta) \rangle$, as a function of the inverse temperature Θ , where the former are the moments, and the latter are the reduced moments of the persistence lengths. We concentrate, in particular, on trails and silhouettes on a square, a triangular, a simple cubic and a face-centered-cubic lattice.

We start by showing analytically that there exist points of inflection in the moments of the persistence lengths, which correspond to the transition temperatures (for a fixed chain length l) of the walk configurations as they collapse from the swollen phase to the compact phase. Plots of $-(\partial/\partial\Theta)\langle X_l^{2k+1}(\Theta) \rangle$ or $-(\partial/\partial\Theta)\langle M_l^{2k+1}(\Theta) \rangle$ of the numerical data exhibit sharp peaks, indicating the existence of the analytically predicted points of inflection. The analytical results are then incorporated with the numerical results to determine the transition temperatures of trails and silhouettes on the four lattices. The values of the transition temperatures obtained from this approach are always lower than those obtained from the specific heats in exact enumerations. Since it is known that specific heats in exact enumerations tend to give a higher Θ for the transition temperatures, our lower values are not unjustified. In fact, our

transition temperatures for trails on the square lattice and the simple cubic lattices are very close to those obtained earlier for much longer chains ($l \sim 220-250$).^{11-13,30}

An interesting observation is that as k (the order of moments) increases, the transition temperature tends to a lower value, even though this is not predicted in the analytical expression [Eq. (8)]. A plausible explanation for this observation is that since our chains are relatively short, chain stiffness may still be strong. This effect tends to increase the persistence lengths. This will push up the value of $\nu(\Theta)$, which in turn causes a lower value of Θ . If we recall that this stiffness is amplified for higher moments, we see that the lowering trend is explained.

On all four lattices, Θ_t for trails are always lower than those for silhouettes. These are in agreement with earlier results.⁷⁻¹⁰ This is explained from the fact that as the temperature is lowered, configurations with loops predominate, and since there is a multiplicity of trails for each silhouette, configurations with loops are more heavily weighted in trails than in silhouettes. Thus energetically, it is more favorable for trails to collapse at a lower Θ (or higher temperature).

For comparison purposes, we have also tabulated in Table I the transition temperatures of trails, silhouettes, and self-attracting SAW's (SA SAW's) on the four lattices. One very clear conclusion that can be extracted from the table is that Θ_t for SA SAW's are always lower than those of the corresponding trails (and thus those of the corresponding silhouettes). This is very easily explained. In SA SAW's, an energy ϵ is associated with each nonbonded nearest neighbor. In trails (silhouettes), an energy ϵ is associated with an intersection. Since nearest neighbors are more abundant, it is not surprising that SA SAW's collapse at a higher temperature (lower Θ). This explanation is further corroborated by the observation $\Theta_t(\text{trails})/\Theta_t(\text{SA SAW's})$ increases as q increases.

In conclusion, we have provided a new criterion for locating the transition temperatures of polymeric models with loops. Our transition temperatures obtained using this criterion for the four lattices, though not determined to very high accuracy, come very close to existing computer-simulation results.^{11-13,32} The results, however, do reflect that close-packed lattices always converge

TABLE I. Transition temperatures on different lattices for the three walk models.

Walk model	Θ_t			
	Square	Triangular	Cubic	fcc
Trails	1.086 ^a	0.4	0.6 ^b	0.3
Silhouettes	1.9	1.2	1.4	0.9
SA SAW's	0.658 ^c	0.4 ^d	0.27 ^e	0.2 ^f

^aReference 13.

^bReference 30.

^cReference 32.

^dReference 33.

^eReference 34.

^fReferences 28 and 35.

faster. The limitation on the accuracy is due to short chains we can generate using exact enumerations. The crux of the enumeration is in the classification of silhouettes, which renders enumerations to very high orders impractical. To date, and to the best of our knowledge, exact enumeration is the only way to classify this type of walk (silhouettes).^{1,2,9,10} Longer chains (trails and silhouettes) will definitely improve the accuracy of the determination of the transition temperatures. In retrospect, the transition temperatures (Θ_t) obtained by this new approach are always lower than their respective specific-heat counter parts. This may be explained as follows: the specific heat, [or in the jargon of statistics, the dispersion of $I_l(\Theta)$] is defined as $h_l(\Theta) = \partial \langle I_l(\Theta) \rangle / (\partial \Theta) = [\langle I_l^2(\Theta) \rangle - \langle I_l(\Theta) \rangle^2]$.^{7-10,28,35} The plot of $\langle I_l(\Theta) \rangle$ versus Θ has a positive slope,³⁵ in contrast to the plot of $\langle X_l^{2k+1}(\Theta) \rangle$ versus Θ (Fig. 3), which has a

negative slope. Because of this, the transition temperatures are approached as an "uphill" (specific heat) or "downhill" (persistence length), and thus in the former, the transition temperatures tend to be a little higher, and in the latter, they tend to be a little lower. In the large chain length limit, this difference is expected to vanish.

ACKNOWLEDGMENTS

The authors are grateful to the Technical Support Group for computing assistance during various stages of the project. The authors also thank the Supercomputer Computations Research Institute for the use of the computer facilities. This work is partially supported by the U.S. Department of Energy under Contract No. DE-FC05-85ER250000, and the Technological Research and Development Authority under Contract No. TRDA No. 103.

¹D. E. Burnette and H. A. Lim, *J. Phys. A* **22**, 3059 (1989).

²D. E. Burnette and H. A. Lim, *J. Phys. A* **22**, 3081 (1989).

³A. Malakis, *J. Phys. A* **8**, 1885 (1975).

⁴A. Malakis, *J. Phys. A* **9**, 1283 (1976).

⁵A. R. Massih and M. A. Moore, *J. Phys. A* **8**, 237 (1975).

⁶Y. Shapir and Y. Oono, *J. Phys. A* **17**, L39 (1984).

⁷H. A. Lim, A. Guha, and Y. Shapir, *J. Phys. A* **21**, 773 (1988).

⁸A. Guha, H. A. Lim, and Y. Shapir, *J. Phys. A* **21**, 1043 (1988).

⁹H. A. Lim, *J. Phys. A* **21**, 3783 (1988).

¹⁰H. A. Lim, A. Guha, and Y. Shapir, *Phys. Rev. A* **38**, 3710 (1988).

¹¹H. Meirovitch and H. A. Lim, *Phys. Rev. A* **38**, 1670 (1988).

¹²H. A. Lim and H. Meirovitch, *Phys. Rev. A* **39**, 4176 (1989).

¹³H. Meirovitch and H. A. Lim, *Phys. Rev. A* **39**, 4186 (1989).

¹⁴D. C. Rapaport, *J. Phys. A* **9**, 1521 (1976).

¹⁵A. J. Guttmann, *J. Phys. A* **18**, 567 (1985).

¹⁶A. J. Guttmann and T. R. Osborn, *J. Phys. A* **21**, 513 (1988).

¹⁷H. Saleur, *Phys. Rev. B* **35**, 3657 (1987), and references therein.

¹⁸G. H. Weiss and R. J. Rubin, *Adv. Chem. Phys.* **32**, 363 (1983).

¹⁹P. J. Flory, *Principles of Polymer Chemistry* (Cornell University Press, Ithaca, 1953).

²⁰H. Yamakawa, *Modern Theory of Polymer Solutions* (Harper

and Row, New York, 1971).

²¹P. G. de Gennes, *Scaling Concepts in Polymer Physics* (Cornell University Press, Ithaca, 1985).

²²M. Doi and S. F. Edwards, *The Theory of Polymer Dynamics* (Clarendon, Oxford, 1986).

²³P. H. Poole, A. Coniglio, N. Jan, and H. E. Stanley, *Phys. Rev. Lett.* **60**, 1203 (1988).

²⁴G. H. Weiss, *J. Math. Phys.* **22**, 562 (1981).

²⁵P. Grassberger, *Phys. Lett.* **89A**, 381 (1982).

²⁶S. Redner and V. Privman, *J. Phys. A* **20**, L857 (1987).

²⁷D. Considine and S. Redner, *J. Phys. A* **22**, 1621 (1989).

²⁸D. C. Rapaport, *J. Phys. A* **10**, 637 (1977).

²⁹*Handbook of Mathematical Functions*, edited by M. Abramowitz and I. A. Stegun (Dover, New York, 1970).

³⁰H. Meirovitch and H. A. Lim (unpublished).

³¹N. W. Ashcroft and N. D. Mermin, *Solid State Physics* (Holt-Saunders, London, 1976), Chap. 4.

³²H. Meirovitch and H. A. Lim, *J. Chem. Phys.* **91**, 2544 (1989).

³³V. Privman and D. A. Kurtze, *Macromolecules* **19**, 2377 (1986).

³⁴H. Meirovitch and H. A. Lim (unpublished).

³⁵J. Mazur, in *Stochastic Processes in Chemical Physics*, edited by K. E. Schuler (Interscience, New York, 1969), p. 261.